Study of the degradation of rolling element bearings with artificial dents

Theo Tselonis[1], Valentius Wirjana[2], Thomas Hughes[3], Zhongxiao Peng[4]

[1-4] *School of Mechanical and Manufacturing Engineering, UNSW Sydney, NSW, 2052, Australia*

theodore.tselonis@ad.unsw.edu.au
v.wirjana@student.unsw.edu.au
thomas.p.hughes@unsw.edu.au
z.peng@unsw.edu.au

ABSTRACT

Contact fatigue in rolling element bearings (REBs) is a common surface degradation and failure mechanism. A better understanding of this process, especially the evolution of tribological features and resultant dynamic responses, is critical for developing effective tools to monitor degradation and predict remaining useful life. This paper investigates the relationship between the geometry of seeded faults – specifically their shape and size – and bearing performance under grease-lubricated conditions. Two bearings with different fault shapes and sizes were tested. To study the degradation process, moulds and images of the fault area were collected at different intervals to capture the gradual progression of wear. The acceleration root mean square (RMS) value of vibrations was used as a real-time indicator to detect significant changes in bearing dynamics throughout the degradation process. This study provides valuable experimental data and insights into the degradation processes of rolling element bearings when they are subjected to initial defects related to manufacturing or contamination, under grease-lubricated conditions. This knowledge is crucial for developing effective real-time techniques for monitoring the degradation process.

1. INTRODUCTION

Rolling contact fatigue (RCF) is a common failure mode in rolling bearings and other mechanical components with rolling and/or sliding motion. RCF is a complex process, involving material properties and surface morphologies of the components in contact (Murakami et al., 1985; Rosado et al., 2010; Branch et al., 2010), operating conditions (e.g., applied load, speed and the slide-to-roll ratio) (Nélias et al., 1999; Rycerz and Kadiric, 2019), lubrication conditions (Halme and Andersson, 2010; Xu et al., 1998) and inclusions/indentations (Nélias and Ville, 2000; Bogdański and Brown, 2002; Kang et al., 2012). Different wear and stress concentration mechanisms can also be involved in the fatigue process (El-Thalji and Jantunen, 2014). Local surface and/or subsurface stress, as determined by the factors mentioned above (Bogdański and Brown, 2002; El Laithy et al., 2019), can initiate cracks or spalls, and influence bearing life (Zaretsky et al., 1996).

It is widely recognised that surface inclusions generated by contamination, damage during manufacturing or installation processes, can act as stress risers which increase local stress and initiate surface degradation (Xu et al., 1998; Ville and Nélias, 1999; Morales-Espejel and Gabelli, 2011, 2015; Golmohammadi and Sadeghi, 2019). Bearing fatigue life reduces when rolling-element or race faults are present as defects that result in higher local tensile residual stress compared to rolling-elements or races without defects. Some experimental works have been conducted investigating the progression of rolling surface damage initiated by dents. For example, round artificially seeded dents, with a diameter of 220 µm and depth of 6.3 µm, were seeded onto the inner raceway of a deep groove ball bearing (type 6205) (Morales-Espejel and Gabelli, 2015). Surface fatigue propagated onto the trailing edge of the dents and formed a V-shape material dislocation. In addition to a round shaped dent, often produced under heavily loaded and pure rolling conditions (Morales-Espejel and Gabelli, 2011), dents of irregular shapes can also be generated elements (comparing element surface or raceway, under rolling and sliding conditions (Ville and Nélias, 1999) and triangular shaped dents caused by impacts from rolling elements (Morales-Espejel and Gabelli, 2015). Existing studies report that dent shapes and sizes can significantly affect fatigue life. In 2016, Makino et al. showed that with a 15-µm diameter defect, the number of rolling contact cycles to flaking life decreased with increasing defect length. The same study revealed that the

defect length did not affect flaking life once it is 50 µm or over. In contrast, it was reported that the shape, size and orientation of an individual inclusion had a relatively minor effect on the fatigue limit (Allison and Pandkar, 2018). With seemingly conflicting findings in the literature, further investigation on the effect of dent shapes and sizes on the fatigue process is required.

The aim of this study is to analyse the impact of artificial defects on REB failure. In particular, it investigates the trend and correlation between the shape and size of seeded dents and the performance and failure of grease-lubricated bearings.

2. METHODOLOGY

The experiment was carried out on UNSW's bearing prognostics simulator, outlined in Ref (Zhang et al., 2022). Two Nachi 6205-2NSE9 deep-groove ball bearings (labelled Bearing A and Bearing B) were tested.

Bearing A tested the evolution of different shaped defects with a 1.00 mm diameter circular with 60 µm depth, 0.50 mm equilateral triangular with 12 µm depth, and a 0.50 mm square dent with 12 µm depth (Figure 1 (a), (b) and (c) respectively). Bearing B tested three circular defects of diameters 0.25 mm, 0.50 mm, and 1.00 mm and dent depths of 12 µm, 30 µm and 60 µm, respectively. An axial load of 12 kN and a rotational speed of 18 Hz were applied to Bearing A. Initially, Bearing B experienced 400k cycles with an axial load of 10 kN with a repeating speed cycle schedule of 6, 10, 12, and 18 Hz with duration of 180 seconds at each frequency.

Before testing, each bearing was disassembled to assess rolling element and race surface quality and finish. They were then lubricated with Castrol 450g Premium Heavy Duty Lithium Grease. The primary goal of each test was to test each bearing until failure, with moulds taken before testing started and every 400k cycle, until significant spikes in RMS vibration values were observed. The vertical and horizontal RMS vibration was measured, in real time, using two B&K 4396 accelerometers positioned on the bearing housing. Any sudden changes in RMS, indicating potential damage, prompted the test to be stopped and the bearing raceway inspected.

To measure the dents and surface damage, a mould was created using Microset 101TH replicating compound. This material was applied on each dent and its surrounding area and left to cure for about 20 minutes. Once the replicating compound was removed, it was taken for imaging and measurement. To capture the surface degradation over time, an Olympus DSX-HRSU (with 100x magnification) and a Keyence vk-x200 series laser scanning confocal microscope (with 100x magnification and 0.50 µm pitch) were used to capture 2D and 3D images, respectively. Once the moulds were taken for each defect and bearing, the bearing was reassembled and regreased for further testing.

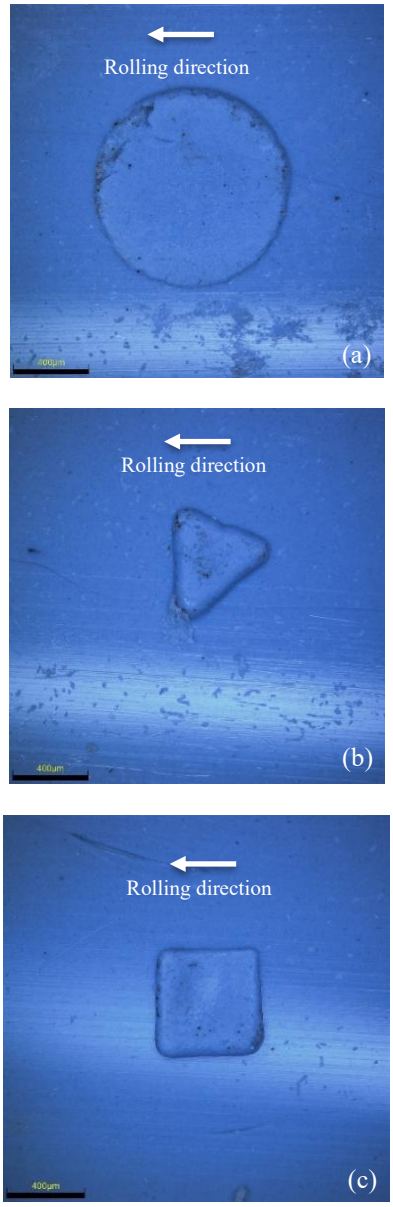

Figure 1. Seeded dents on Bearing A (with motor rotational direction): (a) 1.00-mm diameter circular dent, (b) 0.50-mm equilateral triangle dent, (c) 0.50-mm sided square dent

3. RESULTS

3.1. Bearing A

Bearing A tested three different shaped defects (Figure 1). After 400k cycles, early signs of wear were observed, including uneven surface and edge features (Figure 2(a)) and rounding of edge geometries (Figures 2(b) and 2(c)). This is expected, as local stress concentrations at these points are typically higher than on surfaces farther from the edges. The change observed in the circular dent is the most significant among the three dent types.

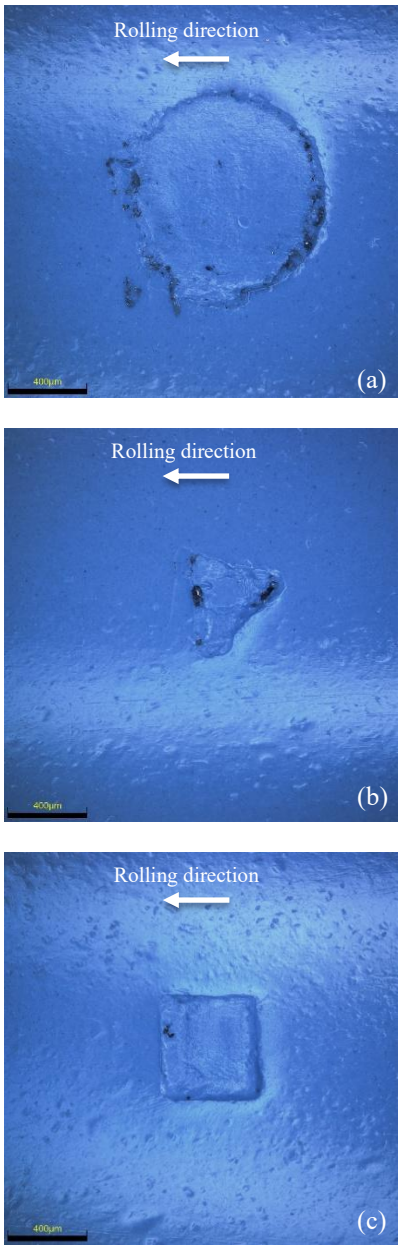

Figure 2. Bearing A at 400k cycles: (a) 1.00-mm diameter circular dent, (b) 0.50-mm sided square dent, (c) 0.50-mm equilateral triangle dent

This bearing was tested for a total of 652k cycles, after which a rapid increase in temperature and RMS vibration was observed, prompting the termination of the test. Figure 3 presents the moulds collected at the end of the test (i.e., at 652k cycles), illustrating the extent of spalling that developed around the dents over time. The circular dent appears to be associated with the most severe surface damage, followed by the triangular dent. Interestingly, the square dent shows minimal surface spalling compared to the circular or triangular dent, likely due to differences in shape.

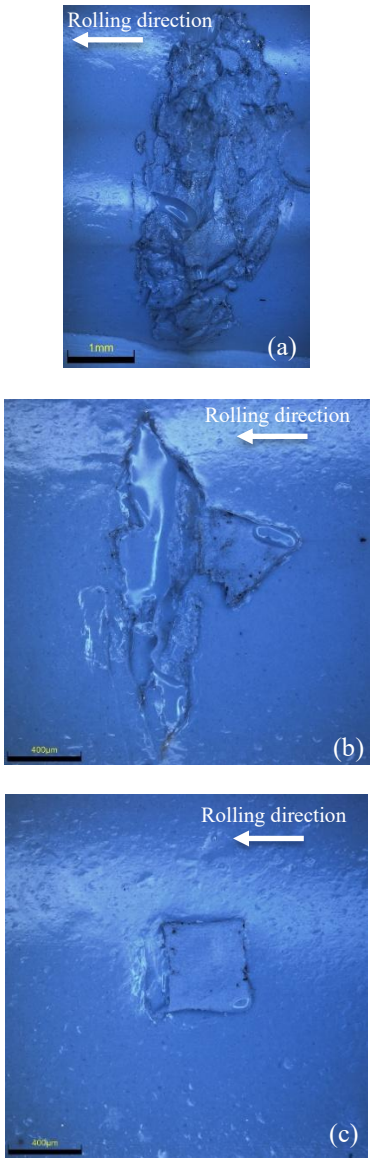

Figure 3. Bearing A at 652 k cycles: (a) 1.00-mm diameter circular dent and surrounding surface spalling, (b) 0.50-mm equilateral triangle dent and surface damage, (c) 0.50-mm square dent

Furthermore, as shown in Figure 3(a), the circular dent exhibited a significant spall area, extending 1849 µm horizontally and 4920 µm vertically beyond the initial dent size in the direction of rolling. Similar to the circular defect, the triangular defect in Figure 3(b) initiated a spall which extended up to 530 µm horizontally and 1547 µm vertically. The square, however, showed a minimal amount of spall evolution compared to the triangular and circular dents. It did show a spall of approximating the height of the initiated fault and extending 140 µm in the direction of rolling. Additionally, a 64-µm long deformation can be observed in the square fault in the bottom right corner.

In addition to the moulds, the RMS values of the vertical and horizontal acceleration of the bearing housing were obtained. The bearing RMS showed significant noise in the measured signals during the test procedure. Figure 4 shows the initial 200k cyles of Bearing A with RMS values averaging 0.11 with a maximum over 0.22. From 200k to 400k cycles the RMS value steadily increased, indicating the initial stages of raceway degradation and the presence of surface damage. Prior to 485k cycles, the RMS averaged around 0.50. Figure 5 shows the mean RMS value at approximately 485k cycles. At that point, it rose sharply to 0.75, with a maximum recorded value approaching 1.5. This increase in RMS continued until 652k cycles (see Figure 6), at which point failure occurred. It is believed that the circular fault played the primary role in the observed rise in RMS acceleration, with the triangular spall contributing secondarily. This is likely due to the spall generated by the circular fault being approximately three times larger than that caused by the triangular fault, and the triangular spall being roughly ten times larger than that produced by the square fault.

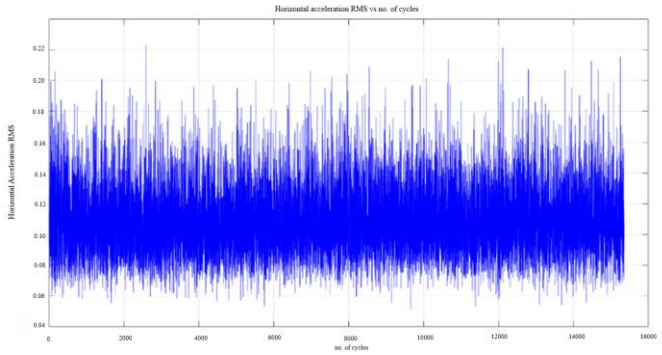

Figure 4. RMS of Bearing A at 200k cycles

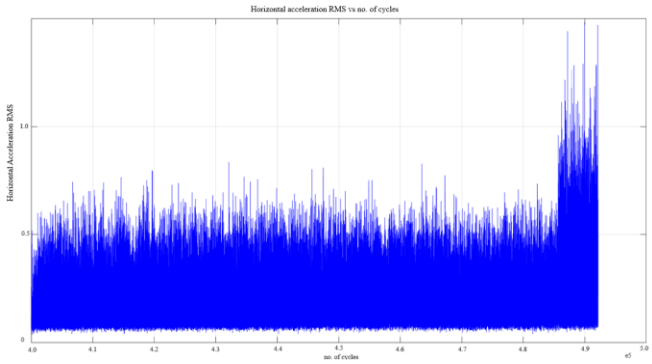

Figure 5. RMS of Bearing A between 400k and 500k cycles

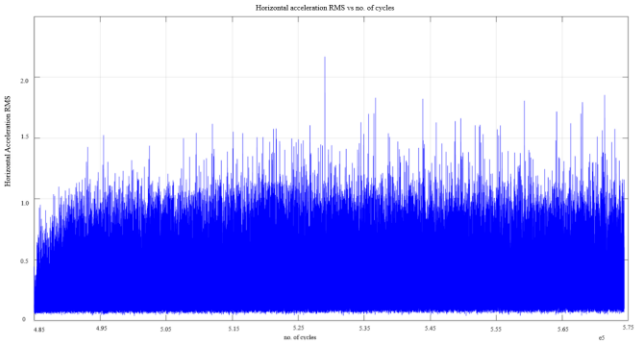

Figure 6. RMS of Bearing A between 485k and 575k cycles.

3.2. Bearing B

Bearing B had three different circular defects and was tested up to 1 million cycles before failure.

The 1.00-mm diameter dent, being the largest among the three tested, was the first to develop a spall and progressed to the most severe degradation condition. Figure 7 shows the evolution of the spall of the 1.00-mm diameter dent. Figure 7(a) shows the initially ovalling and bulging of the circular defect, primarily at the edges of the dent. Figure 7(b) presents the early development of a spall outside the artificial defect, while Figure 7(c) shows the final extent of the spall at the end of the test. After 1 million cycles the maximum spall depth measured was approximately 330 µm. Figure 8 shows the dent conditions of 0.25 mm and 0.5 mm observed at 800k cycles. In comparison to the 1.00-mm dent, only minimal surface damage was observed around the smaller dent area.

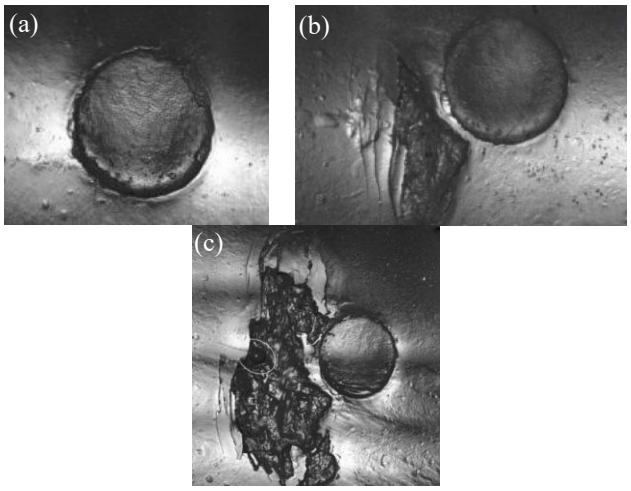

Figure 7. Bearing B with the 1.00-mm diameter dent at (a) 400k cycles, (b) 800k cycles, and (c) 1 million cycles

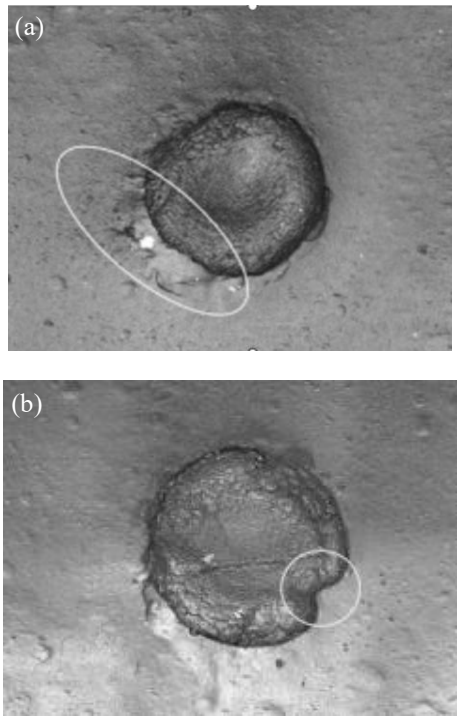

Figure 8. (a) 0.25-mm diameter dent at 800k cycles, (b) 0.50-mm diameter dent at 800k cycles

4. DISCUSSION

4.1. Impact of artificial defect shapes on fatigue

The most extensive damage was present in the 1.00-mm diameter circular dent where a 4920 µm vertically long fault was present after 652k cycles. This follows previous experiments (Zhuang, 2021) the pre-propagation stage would finish at approximately 600k cycles and the propagation stage would begin. This is evident through the change between the sample of the circular and triangular moulds between 400k and 652k. The evolution of deformation around the trailing edge aligned with the findings presented by Cheng et al. (1994), where spalls would first present themselves around the trailing edge due to stress concentrations. The presence of spall development, between 400k and 652k cycles, can be explained by the gradual increase in local bulges and pitting, resulting in uneven stress areas and irregular deformation throughout the surface (Cheng et al., 1994). Similar to the results presented by Cheng et al. (1994) and Zhuang (2021), dent depth contributed to development of rolling contact fatigue (RCF). The circular dent had a greater depth than the triangular and square dents (60 µm vs. 12 µm), and it is likely that this, combined with its shape and diameter, contributed to the development of the largest spall. The triangular dent exhibited signs of damage despite having a smaller size and the same depth as the square dent, which only showed minimal surface damage. It is expected the geometry was the main factor resulting in the differences between the two seeded dents. It is expected that the spall development observed in the experiments followed the physical mechanism outlined in previous research, where the pre-propagation cracks travel below the surface of the bearing and later re-surfaces (Kaneta et al., 2006). Along with the rolling element cycles the applied axial load is expected to accelerate the development of rolling surface abrasions and spalls during the pre-propagation stage. In summary, the circular dent developed the largest spall extent, likely due to its shape, diameter and depth, the triangular dent developed the next largest spall extent, expected to be caused by the shape specifically, finally the square dent presented the least spall extent.

Furthermore, at 400k cycles, both the horizontal and vertical RMS signals began to increase gradually. Then, at 485k cycles, a distinct step change in the measured RMS was observed. It is hypothesised that the primary cause of this step was the sudden evolution of the circular dent spall as this was measured to be the largest when compared to the other two. It is probable that the triangular defect spall also contributed to this step result and the progressive increase in spall size for both circular and triangular fault resulted in the steady increase in RMS observed.

4.2. Impact of artificial defect shapes on fatigue

Seeded dents of three different sizes (diameters and depths of 0.25 mm & 12 µm, 0.50 mm & 30 µm, and 1.00 mm & 60 µm) were tested and compared. All faults exhibited some degree of bulging; however, this was more pronounced in the 0.25 mm and 0.50 mm diameters compared to the 1.00 mm fault, as observed at 800,000 cycles (Figure 7 and 8). The findings from Bearing B indicate that defect size positively correlates with increased fatigue. A comparison of Figure 7(b) with Figures 8(a) and 8(b)—which depict surface damage associated with dents of three different sizes at 800,000 cycles—reveals that faults with larger diameters and greater depths tend to exhibit faster spall evolution relative to the number of cycles the bearing has undergone. Additionally, the depth of the fault has some effect on the surface roughness of the fault surface.

5. CONCLUSION

This paper presents an investigation of RCF in bearings with artificially induced dents. Two sets of bearings were examined, each featuring three different fault configurations. This study observed that surface fatigue initiated by artificial dents progress through two distinct phases: pre-propagation and propagation, regardless of dent shape or size. During the pre-propagation phase, minimal changes in surface morphology were observed. Once spalling begins, the damage area rapidly evolves, resulting in an increase in surface roughness which is reflected in an increase to the measured acceleration RMS signal.

The results of Bearing A indicate that shape and depth of the artificial indentation plays a significant role in bearing

fatigue. The circular fault exhibited the most severe damage, with a fatigue region measuring 4920 μm in length and 1849 μm in width. In contrast, the triangle and square dent showed considerably less RCF over 652k cycles. Furthermore, Bearing B demonstrated that fault diameter was found to be a contributing factor to bearing failure. At 800k cycles, the 1.00-mm dent exhibited extensive spalling, whereas the 0.25-mm and 0.50-mm dents remained in the pre-propagation phase. Overall, the 1.00-mm dent showed the greatest degree of degradation with significant spalling and surface damage. It was determined that a larger dent with a greater depth was more prone to contact fatigue.

In summary, this study offers deeper insight into the surface fatigue process by observing, recording and analyzing the evolution of tribological features and vibration responses in both pre-failure and failure states. The results can provide additional data for the development of effective tools to monitor and predict fatigue progression.

REFERENCES

Allison, B., Pandkar, A. (2018) Critical factors for determining a first estimate of fatigue limit of bearing steels under rolling contact fatigue. Int J Fatigue, 117, 396–406. doi:10.1016/j.ijfatigue.2018.08.004.

Bogdański, S., Brown, M. W. (2002) Modelling the three-dimensional behaviour of shallow rolling contact fatigue cracks in rails. Wear, 253, 17–25. doi:10.1016/S0043-1648(02)00078-9.

Branch, N. A., et al. (2010) Stress field evolution in a ball bearing raceway fatigue spall. J ASTM Int, 7, pages. doi:10.1520/JAI102529.

Cheng, W. H. S. L. M., Cheng, H. S. and Keer, L. M. (1994) Experimental investigation on rolling/sliding contact fatigue crack initiation with artificial defects. Tribology Transactions, 37(1), 1–12.

El Laithy, M., et al. (2019) Further understanding of rolling contact fatigue in rolling element bearings - A review. Tribol Int, 140, 105849. doi:10.1016/j.triboint.2019.105849.

El-Thalji, I., Jantunen, E. (2014) A descriptive model of wear evolution in rolling bearings. Eng Fail Anal, 45, 204–24. doi:10.1016/j.engfailanal.2014.06.004.

Golmohammadi, Z., Sadeghi, F. (2019) A coupled multibody finite element model for investigating effects of surface defects on rolling contact fatigue. J Tribol, 141, pages. doi:10.1115/1.4042270.

Halme, J., Andersson, P. (2010) Rolling contact fatigue and wear fundamentals for rolling bearing diagnostics - State of the art. Proc Inst Mech Eng Part J J Eng Tribol, 224, pages. doi:10.1243/13506501JET656.

Kaneta, M., Nishino, T. and Sakai, T. (2006) A study on surface crack initiation of rolling bearings under rolling–sliding contact. Wear, 261(11–12), 1252–1262.

Kang, J. H., Hosseinkhani, B., Rivera-Díaz-del-castillo, P. E. J. (2012) Rolling contact fatigue in bearings: Multiscale overview. Mater Sci Technol, 28, 44–9. doi:10.1179/174328413X13758854832157.

Makino, T., et al. (2016) Effect of defect shape on rolling contact fatigue crack initiation and propagation in high strength steel. Int J Fatigue, 92, pages. doi:10.1016/j.ijfatigue.2016.02.015.

Morales-Espejel, G. E., Gabelli, A. (2011) The behavior of indentation marks in rolling–sliding elastohydrodynamically lubricated contacts. Tribol Trans, 54, 589–606. doi:10.1080/10402004.2011.582571.

Morales-Espejel, G. E., Gabelli, A. (2015) The progression of surface rolling contact fatigue damage of rolling bearings with artificial dents. Tribol Trans, 58, 418–31. doi:10.1080/10402004.2014.983251.

Murakami, Y., Kaneta, M., Yatsuzuka, H. (1985) Analysis of surface crack propagation in lubricated rolling contact. ASLE Trans, 28, pages. doi:10.1080/05698198508981595.

Nélias, D., et al. (1999) Role of inclusions, surface roughness and operating conditions on rolling contact fatigue. J Tribol, 121, pages. doi:10.1115/1.2833927.

Nélias, D., Ville, F. (2000) Detrimental effects of debris dents on rolling contact fatigue. J Tribol, 122, 55–64.

Rosado, L., et al. (2010) Rolling contact fatigue life and spall propagation of AISI M50, M50NiL, and AISI 52100, part I: Experimental results. Tribol Trans, 53, pages. doi:10.1080/10402000903226366.

Rycerz, P., Kadiric, A. (2019) The influence of slide–roll ratio on the extent of micropitting damage in rolling–sliding contacts pertinent to gear applications. Tribol Lett, 67, pages. doi:10.1007/s11249-019-1174-7.

Ville, F., Nélias, D. (1999) An experimental study on the concentration and shape of dents caused by spherical metallic particles in ehl contacts. Tribol Trans, 42, 231–40. doi:10.1080/10402009908982213.

Xu, G., Sadeghi, F., Hoeprich, M. R. (1998) Dent initiated spall formation in EHL rolling/sliding contact. J Tribol, 120, 453–62. doi:10.1115/1.2834570.

Zaretsky, E. V., Poplawski, J. V., Peters, S. M. (1996) Comparison of life theories for rolling-element bearings. Tribol Trans, 39, 237–48. doi:10.1080/10402009608983525.

Zhang, H., et al. (2022) A benchmark of measurement approaches to track the natural evolution of spall severity in rolling element bearings. Mechanical Systems and Signal Processing, 166, 108466.

Zhuang, S. (2021) Tribological investigation on the degradation process of contact fatigue in rolling bearings. MPhil thesis, UNSW Sydney.